3.5 Ganymede's Aurora

Herbert Gunell, Lorenz Roth, Shahab Fatemi, Chuanfei Dong, and Liang Wang

Abstract

Ganymede, like Earth, has an aurora, but it is hardly observable to the human eye as the dominating wavelengths are in the ultraviolet range. Ganymede is the largest moon of Jupiter, and it has a magnetosphere of its own inside Jupiter's magnetosphere. Ultraviolet emissions have been observed in two bands around the moon, resembling the ovals of Earth's aurora, although at Ganymede they are located at lower latitudes. As the flow of the Jovian magnetospheric plasma around Ganymede is subsonic Ganymede's magnetosphere has no bow shock but instead Alfvén wings develop along the field lines that connect the moon to Jupiter. This interaction not only causes aurora at Ganymede but also at the other end of the field line, where Ganymede's footprint can be seen on Jupiter's auroral oval. At Ganymede, there are indications both of aurora being located at the boundary between the open and the closed field lines of Ganymede's magnetosphere and in regions equatorward of that boundary. Ganymede's aurora appears to have many similarities with Earth's, but the possibility of them being significantly different still remains. Simultaneous observations of the auroral optical emissions and Ganymede's field and plasma environments are necessary to determine what processes are behind Ganymede's aurora and to what extent the physics of it is the same as that of Earth's aurora.

3.5.1 Auroras

We begin this chapter with a discussion of the nature of auroras and how the auroras at Ganymede can be compared to Earth, where the phenomenon has been studied the most. At both Ganymede and Earth the aurora is externally driven. At Earth the energy ultimately comes from the relative motion between the planet and the solar wind, and at Ganymede the energy source is the relative motion between the moon and the plasma in the Jovian magnetosphere. This is another reason for comparing Ganymede to Earth rather than the nearby Jupiter, whose aurora is driven by processes within Jupiter's own magnetosphere.

What is an aurora? The phenomenon was first observed at Earth, where anyone would recognise it, particularly the bright discrete auroral arcs. When light emissions are seen at other bodies, a definition is needed to determine whether or not we may classify them as aurora. A definition is not a law of nature, and reasonable minds may differ on the question of classification. We hold as suitable the proposition that extraterrestrial auroras should look like auroras at Earth and be caused by the same kind of process. The definition we shall adopt here is that the aurora is the light emissions caused by the impact of charged particles from the magnetosphere that precipitate on an atmosphere along the lines of a planetary magnetic field [Knudsen et al., 2021]. This distinguishes aurora from airglow, which is caused by way of local chemistry, and the requirement of a magnetic field sets the aurora apart from other unstructured emissions. It is the magnetic field that leads to the formation of arcs and the large scale organisation into auroral ovals. For comparison we may test this definition by applying it to Mars. Light emissions from the cusps of the Martian crustal magnetic field [Bertaux et al., 2005] are auroras according to our definition, whereas emissions caused by neutral particles [Deighan et al., 2018] or by solar energetic particles [Schneider et al., 2015] are not. One example of an emission at Earth that is not aurora according to our definition is STEVE (Strong Thermal Emission Velocity Enhancement) as that is caused by protons moving horizontally, that is to say, not by field-aligned precipitating particles [Gallardo-Lacourt et al., 2021]. Turning now to our object of interest, Ganymede is itself magnetised (Chapter **2.8:Christensen**) and is thereby surrounded by a small magnetosphere within Jupiter's magnetosphere (Chapter **3.1:Kivelson**). As we shall see below, the emissions come from Ganymede's atmosphere (Chapter **3.3:Roth**) where they form circumpolar bands in regions of vertical magnetic field. They peak in regions with a vertical magnetic field, where models predict the strongest field-aligned current, indicating that the emissions are in agreement with our definition of aurora.

On Earth the aurora is found in ovals around the magnetic poles. The poleward edge of this oval reaches the polar cap boundary, that is to say, the boundary between closed and open field lines. Discrete auroral arcs can at times reach locations near this boundary, and there is an Alfvén Poynting flux going down to the ionosphere and powering this aurora [Keiling et al., 2002], see also the review by Karlsson et al. [2020]. Following the magnetic field lines on the nightside of the planet, this boundary traces the plasma sheet boundary layer all the way to the region of the tail where reconnection takes place [e.g. Akasofu et al., 2010]. However, the vast majority of the aurora is emitted from the part of the ionosphere that is on closed field lines [e.g. Karlsson et al., 2020]. Even during substorms, when bright emissions appear poleward of where the strongest emissions occur, these are equatorward of the open–closed field line boundary [Mauk and Bagenal, 2012].

On Ganymede there is also an open–closed field line boundary, but the magnetospheric configuration differs significantly from that of Earth [Kivelson et al., 1996]. The relative motion of Ganymede and the magnetospheric plasma is slower than the Alfvén speed, and therefore there is no bow shock at Ganymede. On the other hand Alfvén wings emanate from its polar region. These Alfvén wings connect the moon to Jupiter [see also Chapter **3.1:Kivelson** or Kivelson et al., 2002, Neubauer, 1998]. This sub-Alfvénic interaction of Jupiter's magnetospheric plasma with Ganymede's magnetosphere influences the shape and structure of Ganymede's aurora. It leads to an asymmetry, with emissions at higher latitudes on the upstream and lower on the downstream side[1]. As the moon is magnetically connected to Jupiter, the field-aligned potential drops associated with the Alfvén wings accelerate electrons that cause auroras on that planet [e.g. Hess and Delamere, 2012]. When the Juno spacecraft passed above the tail of Ganymede's footprint on Jupiter's ionosphere it was found that Alfvénic acceleration was the dominating electron energisation process [Szalay et al., 2020]. Interaction between Ganymede and Jupiter is treated in Chapter **3.6:Bonfond**.

While there are many sub-categories of aurora at Earth, the two main kinds are the discrete arcs and the diffuse aurora. The discrete arcs are brighter and more localised, but the total precipitated energy of diffuse aurora, integrated over the auroral oval, is higher than that of the discrete arcs [Newell et al., 2009]. In discrete arcs, electrons are accelerated downward by electric fields that are parallel to the magnetic field [e.g. Lysak et al., 2020], whereas in diffuse aurora there is no indication of any such acceleration, instead electrons precipitate after waves have scattered them into the loss cone [e.g. Nishimura et al., 2020]. What drives an auroral arc is not yet completely understood. However, an electric generator mechanism is required to provide the potential drop that accelerates the auroral electrons. A number of generator processes were reviewed recently by Borovsky et al. [2020]. The Juno spacecraft, observing Jupiter's aurora, found electron and ion distributions indicative of both discrete acceleration by electrostatic potential drops and by broadband or stochastic processes. The energy flux was larger for the broadband than the discrete acceleration processes [Mauk et al., 2017]. Juno also observed charged particle distributions indicative of both broadband and discrete acceleration on the same field line in ways that are not known from Earth [Mauk et al., 2018]. For Ganymede even less is known today due to the scarcity of in situ measurements. In this chapter, we review the observations that have been made of aurora at Ganymede, numerical modelling relevant to the aurora, and finally we discuss the open questions and how these can be addressed in coming years.

[1] The speed of Ganymede in its orbit around Jupiter is $\sim 11\,\mathrm{km\,s^{-1}}$, and the corotating plasma of Jupiter's magnetosphere moves at $\sim 150\,\mathrm{km\,s^{-1}}$. Thus, Ganymede is overtaken by the surrounding plasma, and the upstream direction is opposite that of Ganymede's orbital motion.

3.5.2 Observations

Observations of the Ganymede's auroral emissions serve also as the primary observational diagnostic tool for the moon's atmosphere, although detections of an atmosphere has also been made via starlight occultation measurements [Carlson et al., 1973], and an ionosphere was detected through radio occultations by the *Galileo* spacecraft [Kliore, 1998]. For an overview on all aurora observations, we refer to reader to table 1 of Chapter **3.3:Roth** in this book. All listed observations except for the *Galileo* UVS data include the far-ultraviolet oxygen aurora, discussed here.

First detection The first detection of the emissions from Ganymede's oxygen atmosphere, which now generally is called "Ganymede's aurora", were achieved through observations by the Goddard High Resolution Spectrograph (GHRS) of the Hubble Space Telescope (HST) [Hall et al., 1998]. The obtained spectrum (see figure 1 in Chapter **3.3:Roth**) showed atmospheric emissions at the atomic oxygen multiplets near 1304 Å and 1356 Å on top of the surface reflectance signal, similar to the emissions detected on Europa [Hall et al., 1995]. The GHRS data did not provide spatial resolution to map the emissions and Hall et al. [1998] used the term 'airglow' in their study of the observations of the two moons (Europa and Ganymede). 'Airglow' is often used for emissions that originate from energising processes within an atmosphere (e.g., recombination). However, the clear double-peak structure of the OI1356 Å emissions in the Ganymede spectrum allowed Hall et al. [1998] already to speculate about the auroral nature of the Ganymede emissions in the sense of being governed by electron precipitation along magnetic field lines. Indeed, the auroral nature of Ganymede's emissions was later on confirmed, which is distinguished from the neighbouring Callisto, where the faint FUV emissions are thought to originate from photo-electrons ("airglow") [Cunningham et al., 2015].

Static aurora morphology The first images of the oxygen emissions, taken when HST's Space Telescope Imaging Spectrograph (STIS) observed the plasma upstream (orbital trailing) hemisphere of Ganymede in 1998 [Feldman et al., 2000], indeed disclosed an auroral type of topology with brightest emissions clustered near the high latitudes, see Figure 1(c).

Further STIS imaging of the orbital leading hemisphere revealed different oxygen emission morphology with longer bands much closer to the equator (Figure 1a). The images of Ganymede's sub-Jovian hemisphere provide an intermediate vantage point, viewing both the high latitude upstream bands and low latitude downstream bands, with a possible gap in between (Figure 1b).

A comparison to magnetohydrodynamic (MHD) simulations showed that

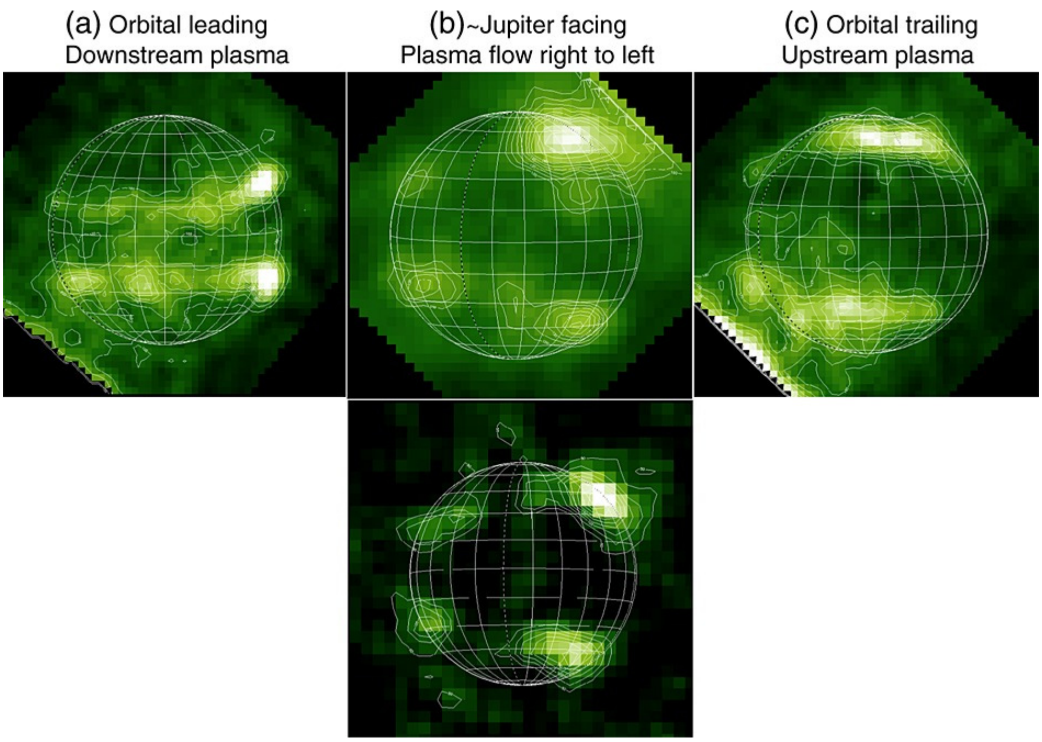

Figure 1: Ganymede's aurora seen from different directions. Both the upper and lower image in the central column are Jupiter-facing but recorded during different observational dates. Figure from [McGrath et al., 2013].

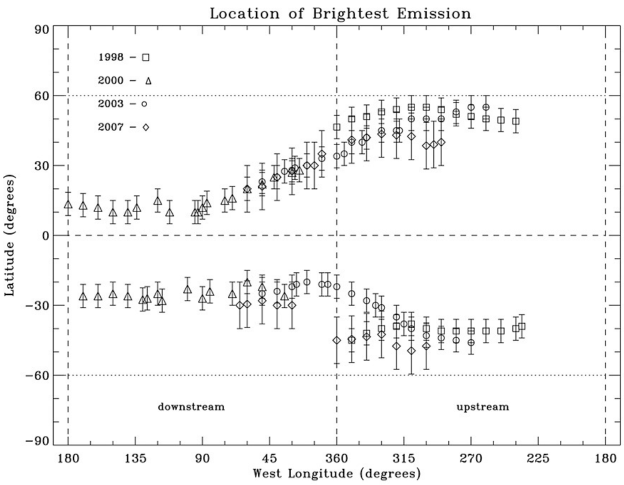

Figure 2: Positions in latitude and longitude of the peak of the emission bands. The different symbols represent the four different observation campaigns. Longitude 0°, or equivalently 360°, is at the centre of Jupiter-facing hemisphere; 90° is facing downstream and 270° upstream. Picture from [McGrath et al., 2013].

the regions of brightest OI 1356 Å emissions are roughly collocated with the open-closed-field-line-boundary (OCFB) of Ganymede's mini-magnetosphere [McGrath et al., 2013]. On the orbital leading side which is also the plasma downstream or wake side, the band-like emissions are close to the equator, as the magnetosphere is stretched. The high-latitude emissions observed on the trailing side, which is also the plasma upstream side, are consistent with a compressed magnetosphere pushing the OCFB further to the poles.

Projections on a latitude-longitude map (Figure 2) suggest that the bright aurora bands can get as close as 10° to the equator on the downstream side and are centred at latitudes 50° N/S on the upstream side. Musacchio et al. [2017] used another approach to quantify the latitude as well as the brightness of the aurora bands by integrating along the horizontal axes in the images, see Figure 3. The peaks of resulting brightness profiles lie between 9° and 28° latitude on the downstream side and upstream close to 50° N/S. Moreover, the study by Musacchio et al. [2017] quantifies an asymmetry in the latitude of the northern and southern bands. Relating this asymmetry in the band latitudes directly to the orientation of Ganymede's dipole magnetic moment, they derive a more westward orientation than the estimations based on in-situ measurement of the magnetic field Kivelson et al. [2002].

The integrated brightness of the 1356 Å emissions in the auroral bands is roughly between 100 R and 200 R (Figure 3), and are generally similar in the more polar upstream (trailing) side and equatorial downstream (leading) side auroral bands. Local peak intensities inside the auroral bands reach ~300 R

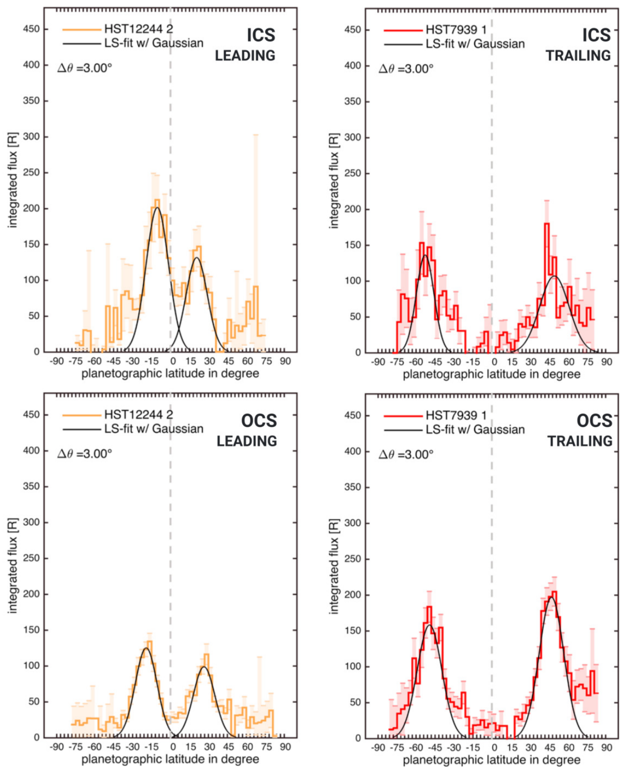

Figure 3: Integrated brightness as function of latitude on both hemispheres when Ganymede is inside the dense plasma or current sheet (ICS) and above or below it (OCS) [Musacchio et al., 2017].

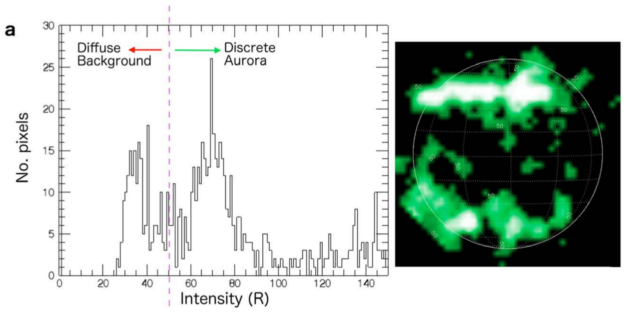

Figure 4: Bright vs. faint or Diffuse vs. discrete aurora [Molyneux et al., 2018]. The purple vertical dashed line in the histogram in the left-hand panel demarcates the threshold over which the emissions were considered bright as opposed to the diffuse background. The image on the right-hand side only includes bright pixels. Pictures from [Molyneux et al., 2018].

[Feldman et al., 2000, McGrath et al., 2013]. The changes in location and brightness (between upper and lower panels in Figure 3) are due to changes in the plasma environment are discussed in Section 3.5.2.

Away from the bright aurora bands, there is a background intensity in the oxygen emissions across the entire disk of about 20-40 R [Feldman et al., 2000, McGrath et al., 2013, Musacchio et al., 2017, Molyneux et al., 2018] (Figure 3, away from peaks). In order to distinguish the emissions from the brighter auroral bands, they are sometimes called "diffuse" emissions (Figure 4). There is, however, no observational constraint on the generating processes and, e.g., on the involved energies of the exciting electron, which would allow a clear separation between different types of auroral emissions across Ganymede. The images of the fainter 1304 Å emissions revealed a generally similar morphology to the 1356 Å emission images [Feldman et al., 2000, Molyneux et al., 2018] with intensities of roughly half the intensity of discussed in the previous paragraph. An analysis of the relative intensities of the two oxygen emissions across the moon disk in images showed that the 1304 Å emissions become relatively stronger towards the sub-solar point [Roth et al., 2021]. This change in the relative emissions originates from contributions of water vapor aurora (dissociative excitation of H_2O) in this region due to sublimation of the ice surface.

Besides the HST observations, Ganymede's aurora was observed by the Pluto-Alice spectrograph onboard the New Horizons spacecraft in 2007. The OI1356 Å intensity measured during two passages of Ganymede through eclipse of Jupiter is presented in Chapter **3.3:Roth**. The stability through eclipse as well as the intensity of the nightside during the second observation confirm that the emissions are independent of solar illumination and thus their auroral nature.

Collinson et al. [2018] analysed ion velocity distributions recorded by the *Galileo* Plasma Subsystem (PLS) during the first flyby of Ganymede by the *Galileo* spacecraft. The authors found downgoing field-aligned ions at the time the spacecraft crossed the OCFB. No electron observations were available as the electron sensors had been damaged by the harsh environment.

Time-variability Although the global appearance of the auroral bands is considered to be relatively stable [McGrath et al., 2013], there are variations of the location of the bands on time-scale of Jupiter's rotation and possibly also temporal variability in the local intensities.

In a dedicated observation campaign, Saur et al. [2015] monitored the auroral bands on the downstream side over half a period of Jupiter's rotation, during two visits in 2010 and 2011. They show that the locations of the auroral bands oscillate due to the periodic oscillation of Jupiter's time-varying magnetic field relative to Ganymede but find that the angle defining the amplitude of this oscillation is only $2.0 \pm 1.3°$. Using resistive MHD simulations they estimated the expected oscillation of the OCFB to be at least $4.5°$. Saur et al. [2015] concluded that a process to reduce the aurora oscillation is required, such as magnetic induction in a sub-surface ocean. The authors assumed that the observed optical emissions coincided with the lines where the OCFB intersects Ganymede's surface, and as discussed in Sect. 3.5.4, this assumption is not yet observationally confirmed. However, for the conclusion of Saur et al. [2015] to hold, collocation of the OCFB and the emissions is not necessarily required. What is necessary is that the two have the same angular oscillation amplitude. To completely confirm this, simultaneous global optical observations and in situ plasma measurements are needed.

Further analysing the variability over the Jupiter rotation, Musacchio et al. [2017] showed that when Ganymede's moves from the denser current sheet ("inside current sheet" or ICS) to more dilute plasma regions above and below ("outside current sheet" or OCS), the emission bands move to lower latitudes on the upstream side and to higher latitudes on the downstream side, as evidenced by comparing the top and bottom rows of Figure 3. These shifts are in accordance with the excepted change of the OCFB in response to plasma density (and thus plasma pressure) changes.

Musacchio et al. [2017] further analyse the evolution of the intensity on average on the disk as well as in the bands over a rotation of Jupiter. On the leading side, both average and band brightness are higher by 30% to 40% when Ganymede is in the plasma sheet centre compared to far outside the plasma sheet (compare top and bottom panel in Figure 3 left). The authors explain this increase with the increased upstream ram pressure, which possibly generates larger magnetic stresses, resulting larger electric currents near the open-closed field line boundary. On the trailing side (top and bottom panel in Figure 3 right), the opposite trend is observed with a decrease by ~20% from the outside-current-sheet (OCS) images to the inside-current-sheet (ICS) images. This is suggested to be caused by a shift of the auroral bands toward the downstream hemisphere (not captured in the image) when the upstream ram pressure is higher (inside the current sheet).

Using later STIS and COS observations from 2014, Molyneux et al. [2018] confirmed these differing brightness changes on the leading and trailing hemisphere. Molyneux et al. [2018] note furthermore that the measured standard deviations of the brightness between individual exposures indicate that there is more temporal variation in the emissions on the leading hemisphere compared to the trailing hemisphere. Systematic changes in the background emissions away from the oval were not found [Musacchio et al., 2017].

3.5.3 Modelling

Modelling of Ganymede's magnetosphere has been performed in the past, using both analytical, fluid and hybrid models. Most of this modelling has not been focused on the aurora, but rather on the larger scale physics of Ganymede's magnetosphere. Photo-chemistry has been used to model dayglow emissions from Ganymede [Cessateur et al., 2016], but that phenomenon is different from the aurora. In this chapter, the analytical models in the next paragraph were used to estimate the auroral emission themselves, whereas the vast majority of the fluid and hybrid models described further below do not include photo-chemistry. The modelled magnetic field has been compared to magnetic field data obtained during the *Galileo* flybys, and improvements in modelling has through the years led to a better ability to reproduce the observed fields. The magnetic field configuration and the physics of the magnetosphere are closely linked to the processes causing the auroral emissions. In this section, we review some of the Ganymede magnetospheric modelling that has been done, while concentrating on the auroral aspects of it.

Analytical models Eviatar et al. [2000] compared electron distributions observed by the *Galileo* spacecraft to analytical models, and it was found that due to an energy dependent injection mechanism mostly high energy electrons are trapped on the closed field lines in Ganymede's magnetosphere. Electron spectrometer energy channels up to 884 keV were considered. Further analytical modelling of both electrons, ions, and neutrals led to the conclusion that there is enough power in the relative motion of Ganymede through Jupiter's magnetosphere to drive the aurora. However, due to the low density of the plasma surrounding Ganymede, an acceleration mechanism in near-Ganymede space is required to achieve the observed auroral intensities [Eviatar et al., 2001b,a]. It was concluded that, although both are possible, acceleration by magnetic field-aligned electric field is more likely than stochastic acceleration by waves [Eviatar et al., 2001a]. Much later, observations by the Juno spacecraft revealed that stochastic acceleration was more important than static electric fields in causing the aurora at Jupiter [Mauk et al., 2017, 2018]. Whether similar discoveries will take place at Ganymede remains to be seen.

Fluid models In global MHD modelling of Ganymede interacting with the plasma of the Jovian magnetosphere, a magnetopause forms upstream of the moon. As Jupiter's and Ganymede's magnetic fields are oppositely oriented reconnection takes place in that region and that is seen in resistive MHD models. These models also reproduce Alfvén wings over Ganymede's polar regions [Ip and Kopp, 2002, Kopp and Ip, 2002]. Furthermore, resistive MHD models predict that field aligned currents run between the region around the OCFB and the Jovian magnetosphere [Ip and Kopp, 2002, Kopp and Ip, 2002] as illustrated in in the top left panel of Fig. 5.

Jia et al. [2008] used resistive MHD to model Ganymede's interaction with the ambient Jovian magnetosphere, and compared the results to the *Galileo* magnetic field measurements. This was improved in a later paper by including models of anomalous resistivity in the reconnection region and an improved ionospheric boundary conditions [Jia et al., 2009]. The enhanced resistivity layer takes on the role of small scale physics that is not explicitly included in the MHD model, and in this way better agreement with observations is reached on a global scale. We see in the lower left panel of Fig. 5 that field aligned currents come from the Alfvén wings reach Ganymede's atmosphere also in this model [Jia et al., 2010], although along a more complicated path than in the earlier simulations by Ip and Kopp [2002] (those shown in the upper left panel of Fig. 5). The flow pattern is shown on the right-hand side of the figure, and in the lower right panel bands of field aligned currents are seen to run across the globe at latitudes approximately corresponding to the location of the auroral ovals. Both upward and downward current regions are seen next to each other, as would be expected in an auroral current circuit. The maxima of the field aligned current density in these resistive MHD models are located on the sides of Ganymede facing Jupiter and away from Jupiter. This should be compared to the configuration of the auroral emissions shown in Fig. 1. There, the emission maxima can be found on the sides leading and trailing the moon in the co-rotating Jovian magnetospheric flow.

The use of Hall MHD to model Ganymede's interaction leads to a magnetospheric configuration that differs from that of resistive MHD. The left panel of Fig. 6 shows the presence of significant plasma flows inside Ga-

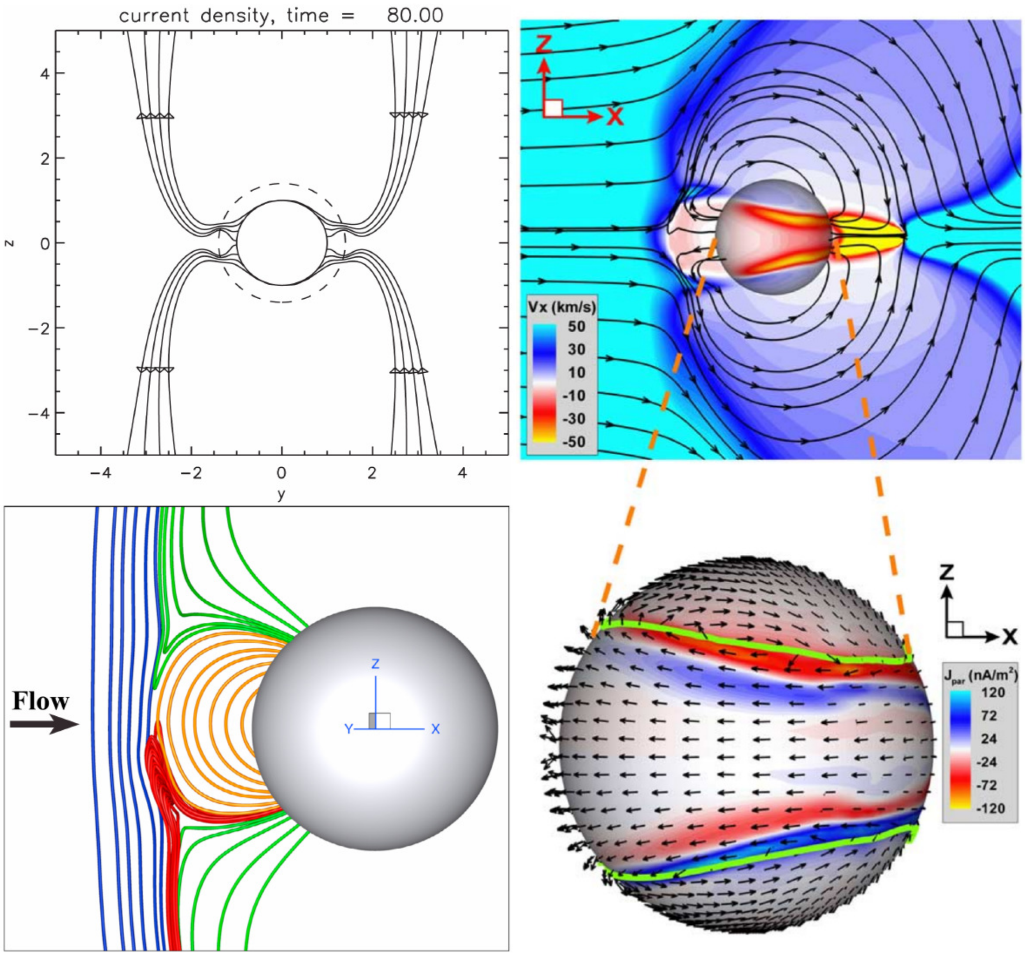

Figure 5: Top left: Field lines connected to the regions with the strongest ionospheric field aligned currents in an MHD simulation [Ip and Kopp, 2002]. The plane shown is perpendicular to the direction of the Jovian magnetospheric plasma flow around Ganymede. Bottom left: field line connectivity in an MHD simulation by Jia et al. [2010]. Top right: Flow pattern in an MHD simulation [Jia et al., 2009]. Bottom right: and field aligned current density at the ionosphere [Jia et al., 2009]. The side of Ganymede shown in the right-hand panels is facing away from Jupiter.

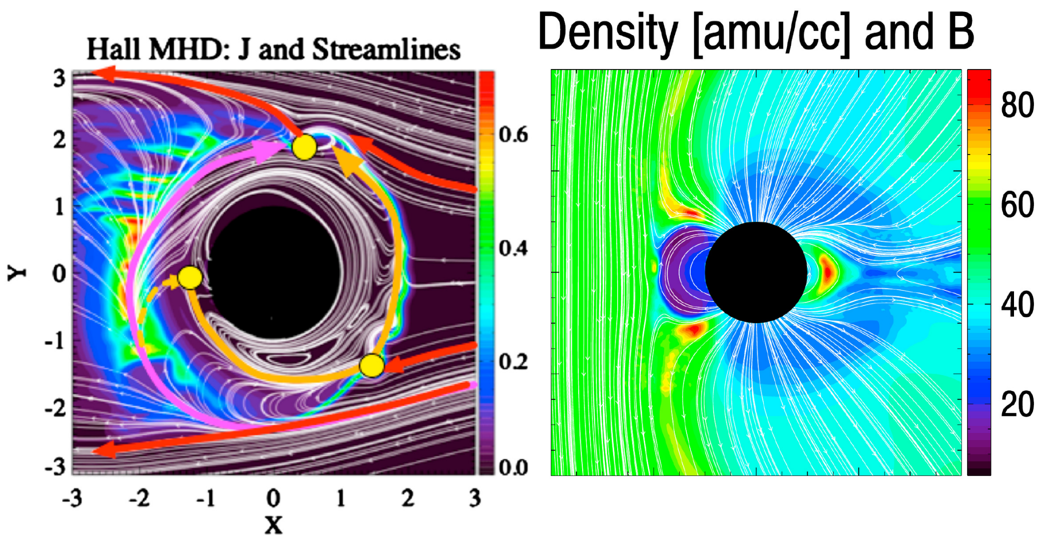

Figure 6: Left: current densities and flow patterns in a Hall MHD simulation [Dorelli et al., 2015]. Right: Densities in a Hall MHD simulation with embedded iPIC patches [Tóth et al., 2016].

nymede's magnetosphere [Dorelli et al., 2015]. At Earth magnetospheric plasma flows are one of the processes that generate field aligned potential drops that in turn accelerate the auroral electrons. As pointed out by Dorelli et al. [2015] to adequately represent field aligned acceleration and electron precipitation into the ionosphere would require a kinetic plasma model. However, the presence of the magnetospheric plasma flows suggests the possibility of an auroral current circuit similar to that of discrete auroral arcs on Earth. Furthermore, the field aligned currents in the Hall MHD simulations connect to Ganymede's ionosphere at the sides leading and trailing in the corotating flow, which corresponds well to where the emissions were observed.

Tóth et al. [2016] used a combined approach: a global Hall MHD simulation where the upstream and tail reconnection regions were were modelled, using an embedded implicit particle in cell code. This could be said to be a hybrid model in that it combines two different approaches to plasma modelling, but it is different from the hybrid models described below in Sect. 3.5.3. The implicit particle in cell model treats both electrons and ions as particles, but it does not resolve the Debye length and the plasma period. A density map produced by this simulation is shown in the right panel of Fig. 6, where the density maximum inside the magnetosphere on the tail, right-hand, side is a feature that is not seen in models based on Hall MHD alone. The plasma density in this region of Ganymede's magnetosphere could influence the auroral current circuits. Zhou et al. [2019] developed this technique further, including an electrical model of Ganymede's interior. From the auroral perspective, the relevant result of the study was the estimate that the energy flux carried by the particles from the reconnection regions down to the atmosphere could account for 40 % of the auroral emissions. Since the regions of space that were modelled using the particle in cell code did not reach down to auroral altitudes this was based on an assumption of constant flux and a calculation of the loss cone. Thus, the possible influence of an acceleration region further below was not taken into account.

Effects similar to those of Hall MHD were also seen in multi-fluid simulations that model more than one ion species [Paty and Winglee, 2004, 2006]. The multi-fluid approach has also been combined with an an auroral brightness model [Payan et al., 2015]. Wang et al. [2018] employed a ten-moment multi-fluid model to study Ganymede–Jovian magnetosphere interaction. A ten-moment model means that it keeps track of ten variables related to the moments of the distribution function for each species: the density, three components of the momentum, and six elements of the pressure tensor. The two fluids modelled represent protons and electrons with a mass ratio of $m_{\mathrm{p}}/m_{\mathrm{e}} = 25$. The results were that high-speed jets flowed from the reconnection regions toward the surface of Ganymede. Figure 7 shows electron (top row) and ion (middle row) scalar pressures mapped onto a sphere 263 km above the surface of the moon. The bottom row shows the emissions observed by the HST [McGrath et al., 2013] for comparison. There is a partial overlap between the electron pressure peak in the northern hemisphere (upper left panel) on the side facing diagonally upstream and away from Jupiter and the light emission shown in the lower left panel. However, apart from that partial overlap, regions with observed light emissions and enhanced simulated electron pressure are disjoint. For the ions, the emission peaks overlap partially with the simulated pressure peaks on the Jupiter facing and downstream sides, but there are also regions where the emissions and ion pressures do not coincide. This emphasises the need for kinetic modelling of the electrons down to ionospheric altitudes.

Hybrid models At the time of this writing, a very few hybrid-kinetic models (particle ions and fluid electrons) have been applied to study the Jovian plasma interaction with Ganymede [Fatemi et al., 2016, Leclercq et al., 2016] or Ganymede-like bodies [Vernisse et al., 2017].

Fatemi et al. [2016] showed the global structure of Ganymede's magnetosphere when Ganymede is inside and outside of the Jovian plasma sheet. They found a good agreement between their simulations and Galileo magnetic field observations during the six close encounters of Ganymede. They also calculated the flux of the Jovian ions precipitating to the surface of Ganymede and found an excellent correlation between the ion precipitation flux and Ganymede's surface brightness patterns. They showed that

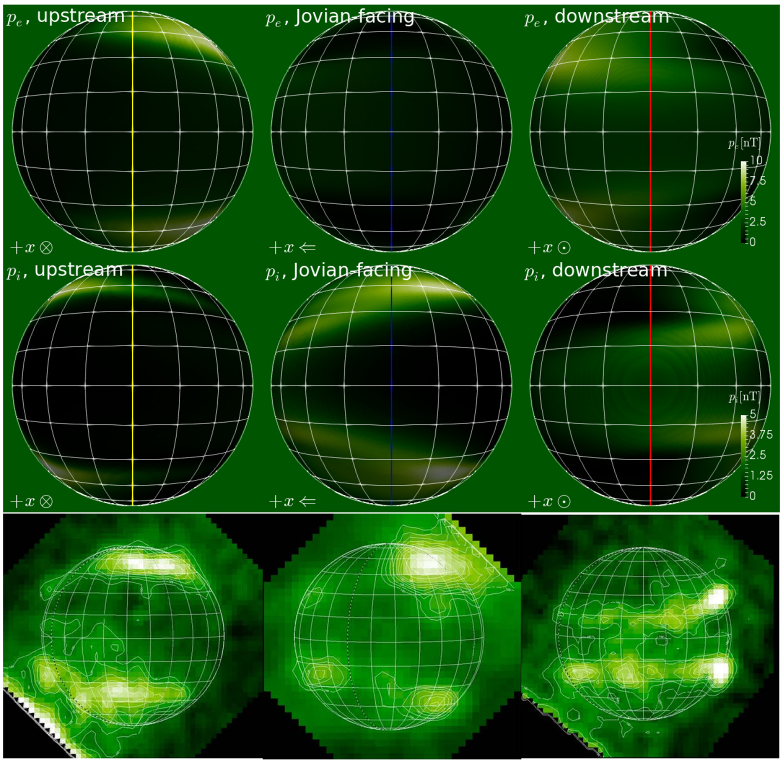

Figure 7: Scalar electron pressure (upper row) and scalar ion pressure (middle row) at 263 km altitude. The left column shows the upstream side; the middle column, the Jupiter facing side; and the right column the downstream side. The yellow, blue, and red curves mark longitudes 270°W, 0°W, 90°W, respectively. The coordinate system was defined by McGrath et al. [2013]. The bottom row shows the light emissions observed by the Hubble Space Telescope [McGrath et al., 2013]. The first two rows and the compilation of the compound figure was made by Wang et al. [2018].

Ganymede's closed magnetic field lines at low latitudes considerably limit the access of the Jovian ions to the surface, while the open field lines over the polar caps facilitate the access of plasma to high latitudes. Leclercq et al. [2016] showed the global structure of Ganymede's magnetosphere as a planetary application of a newly developed method in their hybrid model. The global structure of Ganymede's magnetosphere obtained from their model agrees with previous MHD simulations [e.g. Jia et al., 2008, 2009, Dorelli et al., 2015] and the hybrid simulation by Fatemi et al. [2016], but they did not compare their results with any previous observations.

Precipitating charged particles carry currents, and therefore the current system is relevant to auroral physics [see Baumjohann et al., 2010, for a review of currents in magnetospheres]. Vernisse et al. [2017] applied a hybrid model of plasma to study plasma interaction with magnetised bodies in super-Alfvénic and sub-Alfvénic plasma flow. Their general intention was to investigate the morphology of the current systems and their closure around magnetised bodies. An example of the current systems around a magnetised body (Ganymede-like) that interacts with a sub-Alfvénic plasma flow is shown in Figure 8. The major difference between the modelled body and Ganymede is the orientation of the magnetic dipole moment. Vernisse et al. [2017] have used a southward oriented dipole moment interacting with a southward background magnetic field, while the Ganymede dipole orientation is primarily northward. However, there are similarities between the generated currents in the magnetosphere of the modelled body and those in the magnetosphere of Ganymede. For example, the magnetopause current forms at very close distances to the body, and mainly closes to the Alfvén wing currents. However, the ring current, shown in Figure 8, has not been observed in Ganymede's magnetosphere.

3.5.4 Summary and outlook

What do we know? What do we not know? And how can we find out? Observations by the Hubble Space Telescope have shown emissions of ultraviolet light in bands around Ganymede similar to the auroral ovals on Earth. Observations by the *Galileo* spacecraft made during flybys of Ganymede showed that this moon has an intrinsic magnetic field and a small magnetosphere of its own inside Jupiter's magnetosphere. Furthermore, it is from the auroral observations that we know that Ganymede has an oxygen atmosphere.

Numerical modelling has helped painting a picture of the physical processes behind the aurora at Ganymede. As the plasma flow around the moon is subsonic, no bow shock is formed, instead there are Alfvén wings above the polar regions and the Jovian magnetosphere plasma interacts directly with the magnetopause, where reconnection occurs. The relative motion of

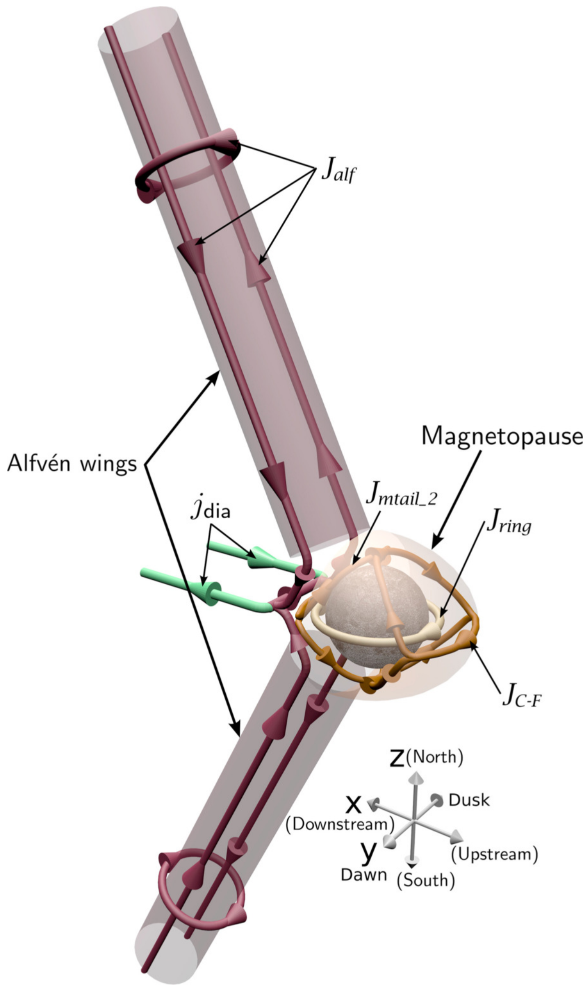

Figure 8: Three-dimensional diagram of the currents systems for a sub-Alfvénic plasma interaction with a magnetised body (Ganymede-like), taken from [Vernisse et al., 2017]. The magnetopause (Chapman-Ferraro) currents are shown in orange, Alvén wing currents are shown in purple, ring currents are in yellow, and the diamagnetic currents are in green.

Ganymede and the surrounding plasma provides the energy that drives the aurora. However, to cause the atmosphere to emit light there must be currents that reach down in the atmosphere and processes that accelerate the electrons downward. In early MHD models, field aligned currents from the Alfvén wings connected directly to the ionosphere at the open–closed field line boundary. Later, models including more of the physics showed more complicated current paths, including plasma flows inside Ganymede's magnetosphere. Such flows may generate field aligned potential drops that can cause electron acceleration on closed field lines, and in turn auroral emissions equatorward of the OCFB. On Earth, this is where the majority of the auroral emissions occur. To simulate these acceleration processes would require kinetic models that can resolve electron scales and that reach all the way down to ionospheric altitudes.

This picture of the physics of Ganymede's aurora is consistent with the observations that have been made, but we cannot say that the observations confirm the picture. We do not have simultaneous observations of the auroral emissions and the magnetic field configuration yet. We do not know from observations what proportion of the aurora is located at the OCFB and how much is generated away from it. We have models of where the field aligned currents are, but we have no direct observations of them. We do not know how the auroral electrons are accelerated or even whether the aurora is dominated by processes similar to discrete arcs or diffuse aurora, both of which are common at Earth. At this time, the physical processes behind Ganymede's aurora are not well constrained by observations.

The upcoming Jupiter icy moons explorer (JUICE) mission from the European Space Agency aims at putting a spacecraft in orbit around Ganymede [Grasset et al., 2013]. This will shed some light upon the outstanding issues. Simultaneously observing emissions, magnetic fields and charged particles should be sufficient to answer the question of where the emissions appear in relation to the different parts of the magnetosphere. Distribution functions of electrons on the field lines that connect to the aurora will provide information about acceleration processes and pitch angle scattering. Observations of cross field plasma flows in the equatorial regions of Ganymede's magnetosphere could be used together with auroral particle observations in the polar regions to put constraints on the parameter space spanned by auroral generators and the auroral current circuit as a whole. To completely understand both the current circuit and the emissions one also need to know the properties of the atmosphere and ionospheres as discussed in Chapters **3.3:Roth** and **3.4:Galand**. All these observations can subsequently be used to put constraints on simulations, both by providing realistic initial and boundary conditions and by telling us which physical processes need be included to obtain results that are consistent with observations. In this way Ganymede auroral modelling will advance to the next level and illuminate the auroral processes of a magnetosphere inside a magnetosphere. This in turn will push the boundaries of our understanding of magnetospheres in general.

Acknowledgements

H. G. was supported by the Swedish National Space Agency (SNSA) grant 108/18. L. R. appreciates the support from the Swedish National Space Agency (SNSA) through grant 154/17 and the Swedish Research Council (VR) through grant 2017-04897. S. F. acknowledges support from the Swedish National Space Agency, grants 179/18 and 115/18, and the Swedish Research Council, grant 2018-03454.

References

Syun-Ichi Akasofu, A. T. Y. Lui, and C.-I. Meng. Importance of auroral features in the search for substorm onset processes. *J. Geophys. Res. (Space Physics)*, 115(A8), 2010. doi:10.1029/2009JA014960.

Wolfgang Baumjohann, Michel Blanc, Andrei Fedorov, and Karl-Heinz Glassmeier. Current systems in planetary magnetospheres and ionospheres. *Space Science Reviews*, 152(1-4):99–134, May 2010. doi:10.1007/s11214-010-9629-z.

J.-L. Bertaux, F. Leblanc, O. Witasse, E. Quemerais, J. Lilensten, S. A. Stern, B. Sandel, and O. Korablev. Discovery of an aurora on Mars. *Nature*, 435:790–794, June 2005. doi:10.1038/nature03603.

Joseph E. Borovsky, Joachim Birn, Marius M. Echim, Shigeru Fujita, Robert L. Lysak, David J. Knudsen, Octav Marghitu, Antonius Otto, Tomo-Hiko Watanabe, and Takashi Tanaka. Quiescent discrete auroral arcs: A review of magnetospheric generator mechanisms. *Space Science Reviews*, 216(1):1, 2020. doi:10.1007/s11214-019-0619-5.

R. W. Carlson, J. C. Bhattacharyya, B. A. Smith, T. V. Johnson, B. Hidayat, S. A. Smith, G. E. Taylor, B. O'Leary, and R. T. Brinkmann. An atmosphere on Ganymede from its occultation of SAO 186800 on 7 June 1972. *Science*, 182(4107):53–55, 1973. ISSN 0036-8075. doi:10.1126/science.182.4107.53.

G. Cessateur, M. Barthelemy, and I. Peinke. Photochemistry-emission coupled model for Europa and Ganymede. *Journal of Space Weather and Space Climate*, 6(27):A17, March 2016. doi:10.1051/swsc/2016009.

Glyn Collinson, William R. Paterson, Christopher Bard, John Dorelli, Alex Glocer, Menelaos Sarantos, and Rob Wilson. New results from Galileo's first flyby of Ganymede: Reconnection-driven flows at the low-latitude magnetopause boundary, crossing the cusp, and icy ionospheric escape. *Geophys. Res. Lett.*, 45(8):3382–3392, 2018. doi:10.1002/2017GL075487.

Nathaniel J Cunningham, John R Spencer, Paul D Feldman, Darrell F Strobel, Kevin France, and Steven N Osterman. Detection of Callisto's oxygen atmosphere with the Hubble Space Telescope. *Icarus*, 254:178–189, 2015.

J. Deighan, S. K. Jain, M. S. Chaffin, X. Fang, J. S. Halekas, J. T. Clarke, N. M. Schneider, A. I. F. Stewart, J. Y. Chaufray, J. S. Evans, M. H. Stevens, M. Mayyasi, A. Stiepen, M. Crismani, W. E. McClintock, G. M. Holsclaw, D. Y. Lo, F. Montmessin, F. Lefèvre, and B. M. Jakosky. Discovery of a proton aurora at Mars. *Nature Astronomy*, 2:802–807, July 2018. doi:10.1038/s41550-018-0538-5.

J. C. Dorelli, A. Glocer, G. Collinson., and G. Tóth. The role of the Hall effect in the global structure and dynamics of planetary magnetospheres: Ganymede as a case study. *J. Geophys. Res. (Space Physics)*, 120:5377–5392, July 2015. doi:10.1002/2014JA020951.

Aharon Eviatar, Donald J. Williams, Chris Paranicas, Richard W. McEntire, Barry H. Mauk, and Margaret G. Kivelson. Trapped energetic electrons in the magnetosphere of Ganymede. *J. Geophys. Res.*, 105(A3):5547–5554, March 2000. doi:10.1029/1999JA900450.

Aharon Eviatar, Darrel F. Strobel, Brian C. Wolven, Paul D. Feldman, Melissa A. McGrath, and Donald J. Williams. Excitation of the Ganymede ultraviolet aurora. *The Astrophysical Journal*, 555(2):1013–1019, July 2001a. doi:10.1086/321510.

Aharon Eviatar, Vytenis M. Vasyliūnas, and Donald A. Gurnett. The ionosphere of Ganymede. *Planet. Space Sci.*, 49(3–4):327–336, March 2001b. doi:10.1016/S0032-0633(00)00154-9.

S Fatemi, AR Poppe, KK Khurana, M Holmström, and GT Delory. On the formation of Ganymede's surface brightness asymmetries: Kinetic simulations of Ganymede's magnetosphere. *Geophys. Res. Lett.*, 43(10): 4745–4754, 2016. doi:10.1002/2016GL068363.

P. D. Feldman, M. A. McGrath, D. F. Strobel, H. W. Moos, K. D. Retherford, and B. C. Wolven. HST/STIS ultraviolet imaging of polar aurora on Ganymede. *The Astrophysical Journal*, 535:1085–1090, June 2000. doi:10.1086/308889.

B. Gallardo-Lacourt, H. U. Frey, and C. Martinis. Proton aurora and optical emissions in the subauroral region. *Space Science Reviews*, 217(1):10, February 2021. doi:10.1007/s11214-020-00776-6.

O. Grasset, M. K. Dougherty, A. Coustenis, E. J. Bunce, C. Erd, D. Titov, M. Blanc, A. Coates, P. Drossart, L. N. Fletcher, H. Hussmann, R. Jaumann, N. Krupp, J.-P. Lebreton, O. Prieto-Ballesteros, P. Tortora, F. Tosi, and T. Van Hoolst. JUpiter ICy moons Explorer (JUICE): An ESA mission to orbit Ganymede and to characterise the Jupiter system. *Planetary and Space Science*, 78:1–21, April 2013. doi:10.1016/j.pss.2012.12.002.

D. T. Hall, D. F. Strobel, P. D. Feldman, M. A. McGrath, and H. A. Weaver. Detection of an oxygen atmosphere on Jupiter's moon Europa. *Nature*, 373(6516):677–679, February 1995.

D. T. Hall, P. D. Feldman, M. A. McGrath, and D. F. Strobel. The far-ultraviolet oxygen airglow of Europa and Ganymede. *The Astrophysical Journal*, 499:475–481, May 1998. doi:10.1086/305604.

S. L. G. Hess and P. A. Delamere. Satellite-induced electron acceleration and related auroras. *Washington DC American Geophysical Union Geophysical Monograph Series*, 197:295–304, January 2012. doi:10.1029/2011GM001175.

Wing-Huen Ip and Andreas Kopp. Resistive MHD simulations of Ganymede's magnetosphere 2. Birkeland currents and particle energetics. *J. Geophys. Res. (Space Physics)*, 107(A12):SMP 42–1–SMP 42–7, 2002. doi:10.1029/2001JA005072.

X. Jia, R. J. Walker, M. G. Kivelson, K. K. Khurana, and J. A. Linker. Three-dimensional MHD simulations of Ganymede's magnetosphere. *J. Geophys. Res. (Space Physics)*, 113:A06212, June 2008. doi:10.1029/2007JA012748.

Xianzhe Jia, Raymond J. Walker, Margaret G. Kivelson, Krishan K. Khurana, and Jon A. Linker. Properties of Ganymede's magnetosphere inferred from improved three-dimensional MHD simulations. *J. Geophys. Res.*, 114(A9):A09209, sep 2009. doi:10.1029/2009JA014375.

Xianzhe Jia, Raymond J. Walker, Margaret G. Kivelson, Krishan K. Khurana, and Jon A. Linker. Dynamics of Ganymede's magnetopause: Intermittent reconnection under steady external conditions. *J. Geophys. Res. (Space Physics)*, 115(A12):A12202, dec 2010. ISSN 0148-0227. doi:10.1029/2010JA015771.

T. Karlsson, L. Andersson, D. M. Gillies, K. Lynch, O. Marghitu, N. Partamies, N. Sivadas, and J. Wu. Quiet, discrete auroral arcs—observations. *Space Science Reviews*, 216(1):16, February 2020. doi:10.1007/s11214-020-0641-7.

A. Keiling, J. R. Wygant, C. Cattell, W. Peria, G. Parks, M. Temerin, F. S. Mozer, C. T. Russell, and C. A. Kletzing. Correlation of Alfvén wave poynting flux in the plasma sheet at 4–7 RE with ionospheric electron energy flux. *J. Geophys. Res. (Space Physics)*, 107(A7):SMP 24–1–SMP 24–13, 2002. doi:10.1029/2001JA900140.

M. G. Kivelson, K. K. Khurana, C. T. Russell, R. J. Walker, J. Warnecke, F. V. Coroniti, C. Polanskey, D. J. Southwood, and G. Schubert. Discovery of Ganymede's magnetic field by the Galileo spacecraft. *Nature*, 384: 537–541, December 1996. doi:10.1038/384537a0.

M. G. Kivelson, K. K. Khurana, and M. Volwerk. The permanent and inductive magnetic moments of Ganymede. *Icarus*, 157:507–522, June 2002. doi:10.1006/icar.2002.6834.

A. J. Kliore. Satellite atmospheres and magnetospheres. In J. Andersen, editor, *Highlights of Astronomy: As Presented at the XXIIIrd General Assembly of the IAU, 1997*, pages 1065–1069. Springer Netherlands, Dordrecht, 1998. ISBN 978-94-011-4778-1. doi:10.1007/978-94-011-4778-1_138.

David J. Knudsen, Joseph E. Borovsky, Tomas Karlsson, Ryuho Kataoka, and Noora Partamies. Editorial: Topical collection on auroral physics. *Space Science Reviews*, 217(1):19, February 2021. doi:10.1007/s11214-021-00798-8.

Andreas Kopp and Wing-Huen Ip. Resistive MHD simulations of Ganymede's magnetosphere 1. time variabilities of the magnetic field topology. *J. Geophys. Res. (Space Physics)*, 107(A12):SMP 41–1–SMP 41–5, 2002. doi:10.1029/2001JA005071.

Ludivine Leclercq, Ronan Modolo, François Leblanc, Sebastien Hess, and Marco Mancini. 3d magnetospheric parallel hybrid multi-grid method applied to planet–plasma interactions. *Journal of Computational Physics*, 309:295–313, 2016. doi:10.1016/j.jcp.2016.01.005.

R. Lysak, M. Echim, T. Karlsson, O. Marghitu, R. Rankin, Y. Song, and T. H. Watanabe. Quiet, discrete auroral arcs: Acceleration mechanisms. *Space Science Reviews*, 216(5):92, July 2020. doi:10.1007/s11214-020-00715-5.

B. H. Mauk, D. K. Haggerty, C. Paranicas, G. Clark, P. Kollmann, A. M. Rymer, S. J. Bolton, S. M. Levin, A. Adriani, F. Allegrini, F. Bagenal, B. Bonfond, J. E. P. Connerney, G. R. Gladstone, W. S. Kurth, D. J. McComas, and P. Valek. Discrete and broadband electron acceleration in Jupiter's powerful aurora. *Nature*, 549(7670):66–69, September 2017. doi:10.1038/nature23648.

B. H. Mauk, D. K. Haggerty, C. Paranicas, G. Clark, P. Kollmann, A. M. Rymer, J. M. Peachey, S. J. Bolton, S. M. Levin, A. Adriani, F. Allegrini, F. Bagenal, B. Bonfond, J. E. P. Connerney, R. W. Ebert, G. R. Gladstone, W. S. Kurth, D. J. McComas, D. Ranquist, and P. Valek. Diverse electron and ion acceleration characteristics observed over Jupiter's main aurora. *Geophys. Res. Lett.*, 45(3):1277–1285, 2018. doi:10.1002/2017GL076901.

Barry Mauk and Fran Bagenal. Comparative auroral physics: Earth and other planets. *Washington DC American Geophysical Union Geophysical Monograph Series*, 197:3–26, January 2012. doi:10.1029/2011GM001192.

M. A. McGrath, X. Jia, K. Retherford, P. D. Feldman, D. F. Strobel, and J. Saur. Aurora on Ganymede. *J. Geophys. Res. (Space Physics)*, 118: 2043–2054, May 2013. doi:10.1002/jgra.50122.

P. M. Molyneux, J. D. Nichols, N. P. N. P. Bannister, E. J. Bunce, J. T. Clarke, S. W. H. Cowley, J.-C. Gérard, D. Grodent, S. E. Milan, and C. Paty. Hubble space telescope observations of variations in Ganymede's oxygen atmosphere and aurora. *J. Geophys. Res. (Space Physics)*, 123(5): 3777–3793, 2018. doi:10.1029/2018JA025243.

Fabrizio Musacchio, Joachim Saur, Lorenz Roth, Kurt D. Retherford, Melissa A. McGrath, Paul D. Feldman, and Darrel F. Strobel. Morphology of Ganymede's FUV auroral ovals. *J. Geophys. Res. (Space Physics)*, 122(3):2855–2876, 2017. doi:10.1002/2016JA023220.

Fritz M. Neubauer. The sub-Alfvénic interaction of the Galilean satellites with the Jovian magnetosphere. *J. Geophys. Res. (Planets)*, 103(E9): 19843–19866, 1998.

P. T. Newell, T. Sotirelis, and S. Wing. Diffuse, monoenergetic, and broadband aurora: The global precipitation budget. *J. Geophys. Res. (Space Physics)*, 114:A09207, September 2009. doi:10.1029/2009JA014326.

Yukitoshi Nishimura, Marc R. Lessard, Yuto Katoh, Yoshizumi Miyoshi, Eric Grono, Noora Partamies, Nithin Sivadas, Keisuke Hosokawa, Mizuki Fukizawa, Marilia Samara, Robert G. Michell, Ryuho Kataoka, Takeshi

Sakanoi, Daniel K. Whiter, Shin-ichiro Oyama, Yasunobu Ogawa, and Satoshi Kurita. Diffuse and pulsating aurora. *Space Science Reviews*, 216 (1):4, January 2020. doi:10.1007/s11214-019-0629-3.

Carol Paty and Robert Winglee. Multi-fluid simulations of Ganymede's magnetosphere. *Geophys. Res. Lett.*, 31(24):L24806, 2004. ISSN 0094-8276. doi:10.1029/2004GL021220.

Carol Paty and Robert Winglee. The role of ion cyclotron motion at Ganymede: Magnetic field morphology and magnetospheric dynamics. *Geophys. Res. Lett.*, 33(10), may 2006. ISSN 00948276. doi:10.1029/2005GL025273.

A. P. Payan, C. S. Paty, and K. D. Retherford. Uncovering local magnetospheric processes governing the morphology and variability of Ganymede's aurora using three-dimensional multifluid simulations of Ganymede's magnetosphere. *J. Geophys. Res. (Space Physics)*, 120(1): 401–413, jan 2015. ISSN 21699380. doi:10.1002/2014JA020301.

Lorenz Roth, Nickolay Ivchenko, G. Randall Gladstone, Joachim Saur, Denis Grodent, Bertrand Bonfond, Philippa M. Molyneux, and Kurt D. Retherford. A sublimated water atmosphere on Ganymede detected from Hubble Space Telescope observations. *Nature Astronomy*, July 2021. doi:10.1038/s41550-021-01426-9.

J. Saur, S. Duling, L. Roth, X. Jia, D. F. Strobel, P. D. Feldman, U. R. Christensen, K. D. Retherford, M. A. McGrath, F. Musacchio, A. Wennmacher, F. M. Neubauer, S. Simon, and O. Hartkorn. The search for a subsurface ocean in Ganymede with Hubble Space Telescope observations of its auroral ovals. *J. Geophys. Res. (Space Physics)*, 120:1715–1737, March 2015. doi:10.1002/2014JA020778.

N. M. Schneider, J. I. Deighan, S. K. Jain, A. Stiepen, A. I. F. Stewart, D. Larson, D. L. Mitchell, C. Mazelle, C. O. Lee, R. J. Lillis, J. S. Evans, D. Brain, M. H. Stevens, W. E. McClintock, M. S. Chaffin, M. Crismani, G. M. Holsclaw, F. Lefevre, D. Y. Lo, J. T. Clarke, F. Montmessin, and B. M. Jakosky. Discovery of diffuse aurora on Mars. *Science*, 350:0313, November 2015. doi:10.1126/science.aad0313.

J. R. Szalay, F. Allegrini, F. Bagenal, S. J. Bolton, B. Bonfond, G. Clark, J. E. P. Connerney, R. W. Ebert, D. J. Gershman, R. S. Giles, G. R. Gladstone, T. Greathouse, G. B. Hospodarsky, M. Imai, W. S. Kurth, S. Kotsiaros, P. Louarn, D. J. McComas, J. Saur, A. H. Sulaiman, and R. J. Wilson. Alfvénic acceleration sustains Ganymede's footprint tail aurora. *Geophysical Research Letters*, 47(3):e2019GL086527, 2020. doi:10.1029/2019GL086527.

Gábor Tóth, Xianzhe Jia, Stefano Markidis, Ivy Bo Peng, Yuxi Chen, Lars K S Daldorff, Valeriy M. Tenishev, Dmitry Borovikov, John D. Haiducek, Tamas I. Gombosi, Alex Glocer, and John C. Dorelli. Extended magnetohydrodynamics with embedded particle-in-cell simulation of Ganymede's magnetosphere. *J. of Geophys. Re. A: Space Physics*, 121(2):1273–1293, feb 2016. ISSN 21699402. doi:10.1002/2015JA021997.

Y Vernisse, JA Riousset, U Motschmann, and K-H Glassmeier. Stellar winds and planetary bodies simulations: Magnetized obstacles in super-Alfvénic and sub-Alfvénic flows. *Planetary and Space Science*, 137:40–51, 2017. doi:10.1016/j.pss.2016.08.012.

Liang Wang, Kai Germaschewski, Ammar Hakim, Chuanfei Dong, Joachim Raeder, and Amitava Bhattacharjee. Electron physics in 3-D two-fluid 10-moment modeling of Ganymede's magnetosphere. *J. Geophys. Res. (Space Physics)*, 123(4):2815–2830, 2018. doi:10.1002/2017JA024761.

Hongyang Zhou, Gábor Tóth, Xianzhe Jia, Yuxi Chen, and Stefano Markidis. Embedded kinetic simulation of ganymede's magnetosphere: Improvements and inferences. *J. Geophys. Res. (Space Physics)*, 124(7): 5441–5460, 2019. doi:10.1029/2019JA026643.